

Adolescent Feline Heart Contains a Population of Small, Proliferative Ventricular Myocytes With Immature Physiological Properties

Xiongwen Chen,* Rachel M. Wilson,* Hajime Kubo, Remus M. Berretta, David M. Harris, Xiaoying Zhang, Naser Jaleel, Scott M. MacDonnell, Claudia Bearzi, Jochen Tillmanns, Irina Trofimova, Toru Hosoda, Federico Mosna, Leanne Cribbs, Annarosa Leri, Jan Kajstura, Piero Anversa, Steven R. Houser

Abstract—Recent studies suggest that rather than being terminally differentiated, the adult heart is a self-renewing organ with the capacity to generate new myocytes from cardiac stem/progenitor cells (CS/PCs). This study examined the hypotheses that new myocytes are generated during adolescent growth, to increase myocyte number, and these newly formed myocytes are initially small, mononucleated, proliferation competent, and have immature properties. Ventricular myocytes (VMs) and cKit⁺ (stem cell receptor) CS/PCs were isolated from 11- and 22-week feline hearts. Bromodeoxyuridine incorporation (in vivo) and p16^{INK4a} immunostaining were measured to assess myocyte cell cycle activity and senescence, respectively. Telomerase activity, contractions, Ca²⁺ transients, and electrophysiology were compared in small mononucleated (SMMs) and large binucleated (LBMs) myocytes. Heart mass increased by 101% during adolescent growth, but left ventricular myocyte volume only increased by 77%. Most VMs were binucleated (87% versus 12% mononucleated) and larger than mononucleated myocytes. A greater percentage of SMMs was bromodeoxyuridine positive (SMMs versus LBMs: 3.1% versus 0.8%; *P*<0.05), and p16^{INK4a} negative and small myocytes had greater telomerase activity than large myocytes. Contractions and Ca²⁺ transients were prolonged in SMMs versus LBMs and Ca²⁺ release was disorganized in SMMs with reduced transient outward current and T-tubule density. The T-type Ca²⁺ current, usually seen in fetal/neonatal VMs, was found exclusively in SMMs and in myocytes derived from CS/PC. Myocyte number increases during adolescent cardiac growth. These new myocytes are initially small and functionally immature, with patterns of ion channel expression normally found in the fetal/neonatal period (*Circ Res.* 2007;100:536-544.)

Key Words: new ventricular myocytes ■ T-type calcium current ■ cardiac stem cells ■ calcium

The possibility that resident progenitor cells are present in the developing and adult heart¹ suggests that new myocytes are continuously formed to replace dying cells. Based on this paradigm, a positive balance with a prevailing generation of myocytes would be expected to occur during the transition from the adolescent to the adult heart phenotype to accommodate the increase in body mass, blood flow, and cardiac workload. To support this dynamic view of the heart, a significant degree of structural and functional myocyte heterogeneity should be present during periods of cardiac growth.

Myocyte maturation involves a progressive increase in cell size and structural complexity² that is coupled with the loss of replicative potential.³ Conversely, recently formed myocytes

may have the properties of small amplifying, functionally immature cells that retain the ability to divide and concurrently differentiate.¹ At the completion of this process, myocytes become terminally differentiated and can only undergo cellular hypertrophy.⁴ As myocytes become hypertrophic and senescent, they may die by apoptosis.⁵

To test whether this emerging model of cardiac biology holds merit and might be applicable to large mammals including humans, we determined the cellular mechanisms implicated in the increase in mass of the adolescent feline heart. Myocyte formation, myocyte hypertrophy, and myocyte apoptosis were concurrently examined because cell death, cell regeneration, and cell differentiation modulate tissue homeostasis and growth in self-renewing organs regu-

Original received November 10, 2006; revision received January 8, 2007; accepted January 22, 2007.

From the Cardiovascular Research Center (X.C., R.M.W., H.K., R.M.B., N.J., S.M.M., S.R.H.), Temple University School of Medicine, Philadelphia, Pa; Center for Translational Medicine (D.M.H.), Department of Medicine, Thomas Jefferson University, Philadelphia, Pa; Fox Chase Cancer Center (X.Z.), Philadelphia, Pa; Cardiovascular Research Institute (C.B., J.T., I.T., T.H., F.M., A.L., J.K., P.A.), Department of Medicine, New York Medical College, Valhalla; and Department of Medicine (L.C.), Cardiovascular Institute, Loyola University Medical Center, Maywood, Ill.

*Both authors contributed equally to this study.

Correspondence to Dr Steven R. Houser, Cardiovascular Research Center, Temple University School of Medicine, 3400 North Broad St, Philadelphia, PA 19140. E-mail shouser@temple.edu

© 2007 American Heart Association, Inc.

Circulation Research is available at <http://circres.ahajournals.org>

DOI: 10.1161/01.RES.0000259560.39234.99

lated by a pool of resident progenitor cells.⁵ The possibility that these fundamental cellular processes are operative in the maturing and adult myocardium raises some critical questions concerning the presence and functional integration of newly formed immature myocytes together with adult terminally differentiated and senescent cells.¹ By inference, the electrophysiological, contractile, and Ca^{2+} handling properties of these classes of parenchymal cells may be profoundly distinct.¹ This variability in myocyte function predicts an unprecedented dynamism of the heart and poses complex questions about the cellular physiological basis of ventricular performance.

The hypotheses tested in the present research are that myocyte number increases during normal adolescent cardiac growth and these newly formed myocytes are functionally immature. The respective contributions of myocyte growth (hypertrophy) and increased myocyte number (hyperplasia) to the increase in cardiac mass during normal adolescent growth was determined. Newly formed myocytes were identified by bromodeoxyuridine (BrdUrd) incorporation and markers of cell cycle activity, and then the electrophysiological, contractile, and Ca^{2+} handling properties of new versus mature myocytes were compared. As an initial step toward determining the source of these new myocytes, we also studied whether the young adult feline heart contains a resident cKit⁺ (stem cell factor) cardiac stem/progenitor cell (CS/PC) that can differentiate into new cardiac myocytes (in vitro).

Our results show that the increase in the mass of the adolescent feline heart involves an increase in both myocyte size and number. BrdUrd was incorporated into a small percentage of cardiac myocytes, with preferential incorporation into small mononucleated myocytes (SMMs) that also expressed markers of cell cycle activity (Ki67) and had greater telomerase activity than large binucleated myocytes (LBMs). SMMs had a less organized T-tubular system and more slowly rising, prolonged Ca^{2+} transients than LBMs. In addition, SMMs uniquely expressed T-type Ca^{2+} channels (TTCCs), which are involved in the differentiation and proliferation^{6,7} of other cell types. We also found that the normal feline heart contains a population of resident c-Kit⁺ CS/PCs that, when cocultured with rat neonatal myocytes, differentiate into cardiac myocytes that also express T-type Ca^{2+} currents. These data strongly support the idea that cardiac myocyte number increases during adolescent growth, with newly formed myocytes initially having immature physiological properties.

Materials and Methods

Ventricular myocytes (VMs)⁸ and CS/PCs⁹ were isolated from adolescent feline hearts. BrdUrd incorporation,¹⁰ nucleation, and cell volume^{11,12} were determined in isolated myocytes. Myocyte surface area, Ki67 expression,¹³ p16ink4a expression,⁵ telomerase activity,¹³ and structural¹⁴ and functional properties^{15,16} were compared in small mononucleated myocytes versus in binucleated ventricular myocytes.

An expanded Materials and Methods section can be found in the online data supplement at <http://circres.ahajournals.org>.

Results

Heart Size Increases More Than Myocyte Size During Adolescent Growth

Heart mass of adolescent felines increased by 101% between 11 and 22 weeks of age (7.46 ± 0.28 g [N=6] versus 14.98 ± 0.18 g [N=16]; $P < 0.001$). Myocyte volume fraction did not change during this time ($81.8 \pm 0.66\%$ at 11 weeks and $80.9 \pm 0.9\%$ at 22 weeks, $n=3$ at both ages). If no new myocytes were generated during adolescent growth, then myocyte volume should increase by 101%. Myocyte volume, determined by Coulter Z2 particle size analysis,¹¹ using populations of isolated cells, increased from $11\,782 \pm 438$ to $20\,871 \pm 909$ μm^3 in these hearts, a 77% increase ($P < 0.005$). Identical increases in myocyte volume during adolescent growth were found by measuring myocyte 2D surface area and cell depth (with confocal microscopy) and then computing myocyte volume¹² (see below). Collectively, these data show that the increase in myocyte size during adolescent cardiac growth is not sufficient to account for the associated increase in cardiac mass, consistent with the hypothesis that new myocytes are generated during adolescent growth and result in an increase in myocyte number.

Number and Size of Mononucleated and Binucleated Ventricular Myocytes

The adolescent (11-week) and young adult (22-week) feline hearts had a significantly greater percentage of binucleated ($87.3 \pm 1.2\%$) than mononucleated ($11.5 \pm 1.3\%$) left ventricular myocytes (23 280 myocytes from 12 hearts; Figure 1A). No difference in nucleation was detected at 11 versus 22 weeks. The size of these 2 myocyte populations was significantly different in both adolescent and young hearts. Two dimensional surface area (SA) (Figure 1) and cell depth of mononucleated myocytes were significantly smaller than that of binucleated myocytes from the adolescent (11 weeks) hearts (SA = 1262.19 ± 65.55 μm^2 [$n=157$] in mononucleated versus SA = 2007.14 ± 111.58 μm^2 [$n=333$] in binucleated; $N=3$; $P < 0.0001$; cell depth = 4.99 μm in mononucleated and cell depth = 5.83 μm in binucleated myocytes; $P < 0.01$) and the young adult (22 weeks) hearts (SA = 1534.41 ± 25.44 μm^2 [$n=573$] in mononucleated versus SA = 2566.26 ± 43.20 μm^2 [$n=1250$] in binucleated; $N=11$; $P < 0.0001$; Figure 1A; cell depth = 6.65 ± 0.14 μm [$n=31$] in mononucleated myocytes and cell depth = 7.76 ± 0.09 μm [$n=34$] in binucleated myocytes; $P < 0.01$). The myocyte volume calculated from these morphological measurements was $10\,921.8$ μm^3 in the 11-week hearts and increased by 70% in the 22-week feline hearts ($18\,558.5$ μm^3). These average myocyte volumes are almost identical to those determined by Coulter analysis. Because mononucleated myocytes were significantly smaller than binucleated myocytes, we refer to mononucleated myocytes as small mononucleated myocytes (SMMs) and binucleated myocytes as large binucleated myocytes (LBMs).

Bromodeoxyuridine Incorporation in Adolescent Ventricular Myocytes

The percentage of BrdUrd⁺ mono- and binucleated myocytes was measured (Figure 1A) on VMs isolated from adolescent (22-week-old) animals in which BrdUrd minipumps had been

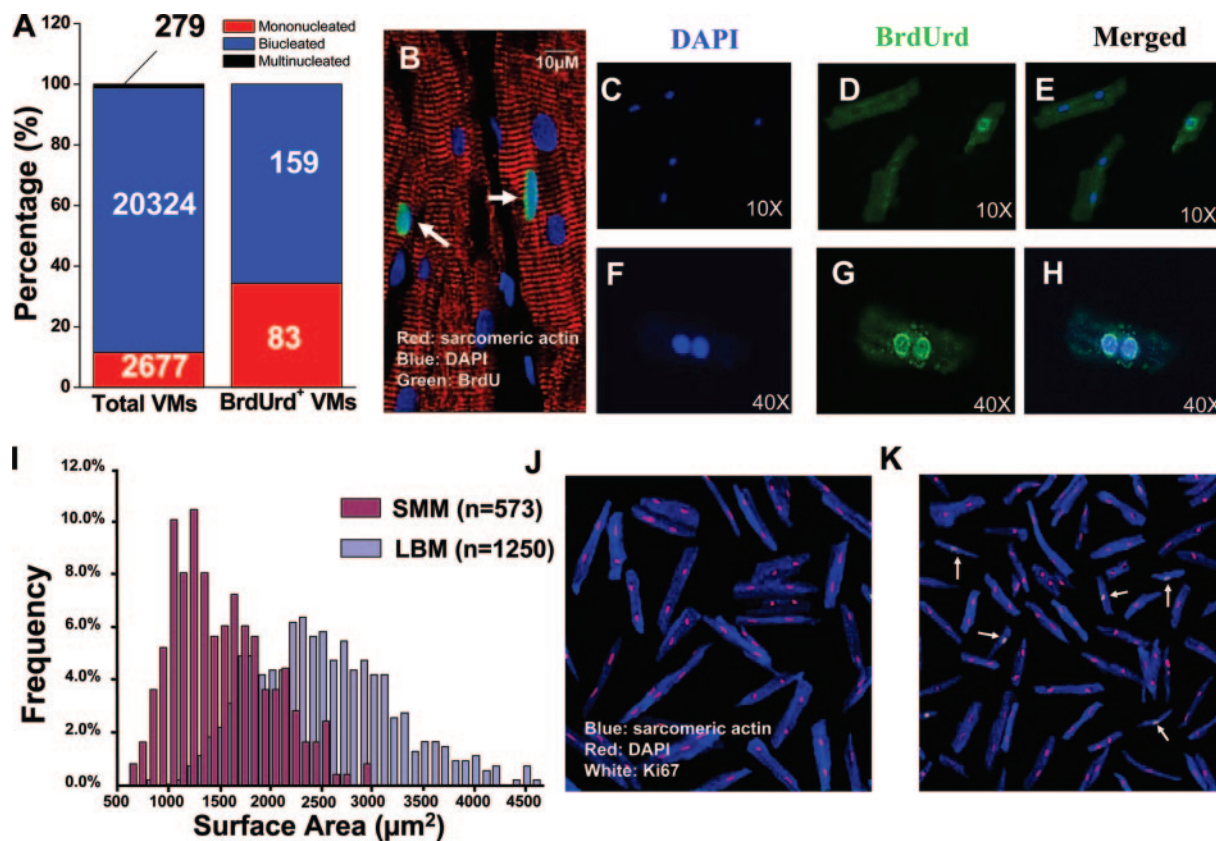


Figure 1. Nucleation, BrdUrd incorporation, surface area, and Ki67 expression in VMs isolated from normal adolescent feline hearts. A, The percentage of mono-, bi-, and multinucleated cells in all VMs (left) and BrdUrd⁺ VMs (right) isolated from 22-week hearts are shown. Numbers in the graph are the numbers counted for these hearts. B through H, Myocyte BrdUrd incorporation in tissue sections (B) (red, sarcomeric actin; blue, 4'-6-diamidino-2-phenylindole [DAPI]; green, BrdUrd; white arrows, BrdUrd⁺ nuclei) and in both mononucleated (C, D, and E) and binucleated (F, G, and H) VMs (blue, DAPI; green, BrdUrd). BrdUrd⁺ VMs were smaller than BrdUrd⁻ VMs. I, The frequency distribution of the surface area of mononucleated (red) and binucleated (blue) myocytes. J and K, Ki67 was mainly found in SMMs (K) vs LBMs (J). Magenta indicates DAPI; blue, cardiac actin; white, Ki67; white arrows, Ki67⁺ myocytes.

inserted (7 days of subcutaneous infusion; 10 mg/kg per day). BrdUrd incorporation was observed in myocyte nuclei in tissue sections (Figure 1B), but the percentage of BrdUrd⁺ nuclei was quantified in isolated myocytes, so that we could unambiguously determine whether these cells were mono- or binucleated. The percentage of BrdUrd⁺ isolated myocytes was 1.04% (242/23 280 myocytes; N=12 hearts), but a greater percentage of mononucleated ($3.1 \pm 0.8\%$) than binucleated ($0.8 \pm 0.4\%$) myocytes were found ($P=0.01$; N=12 hearts) (Figure 1A and 1C through 1H). Ki67 staining was observed in a small percentage of myocytes, and the majority (>95%) of these were small mononucleated myocytes (Figure 1J and 1K). These studies strongly support the idea that new myocytes are generated in the normal young adult heart and that these myocytes are small and mononucleated.

The number of myocytes within the 11- and 22-week hearts computed^{11,12} using measured myocyte volumes (Coulter or morphological measurements), heart weights, and myocyte volume fraction increased from 5.48×10^8 to 6.16×10^8 , consistent with an average increase in new myocytes of 8.8×10^5 per day. Incrementing myocyte number in the 11-week heart by 1.04% per week (the percentage of BrdUrd⁺ myocytes per week) for 11 weeks predicts that the

myocyte number will increase to 6.11×10^8 , almost identical to the number determined independently by morphological analyses.

Senescence Markers and Telomerase Activity in Small Versus Large Ventricular Myocytes

Newly formed small mononucleated myocytes would be expected to be “younger” than their binucleated counterparts. This idea was explored by staining ventricular myocytes for the cell senescence marker p16^{INK4a} (Figure 2A and 2B).⁵ A small fraction of these myocytes were p16^{INK4a+} in 11- and 22-week hearts (8.1% and 7.1%, respectively), and most (>95%) were LBMs.

Newly formed myocytes might also retain the ability to proliferate. To test this idea, isolated myocytes were separated by size and the telomerase activity of small and large myocytes was measured. This assay was performed because telomerase activity is commonly found in activated stem cells and early committed cells undergoing rapid growth and differentiation.⁵ In fact, when cells are mature, they became telomerase incompetent and the downregulation of the catalytic function of the ribonucleoprotein is a necessary step for the acquisition of the terminally differentiated phenotype.⁵ Telomerase activity was observed in all myocyte populations but was significantly higher in the pool of smallest myocytes

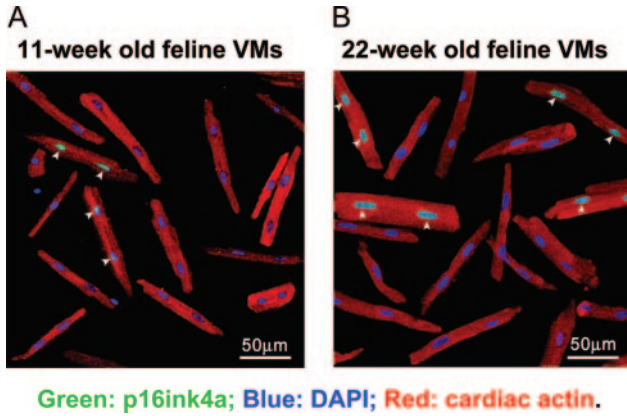


Figure 2. P16^{INK4a} immunostaining in adolescent feline myocytes. p16^{INK4a} immunostaining was primarily observed in LBMs in 11-week (A) and 22-week (B) myocytes.

obtained from 5 cat hearts at 22 weeks of age (Figure 3A and 3B). The enhanced enzyme activity in small myocytes is consistent with the higher level of cell replication documented in this cell subset by BrdUrd incorporation and Ki-67 labeling. Telomere length (QFISH) was not significantly different in 11-week (20.2±2.4kb) and 22-week (20.9±3.1kb) myocytes, consistent with telomerase-dependent preservation of telomere length in these young animals.

Apoptosis in the Adolescent Heart

An increase in myocyte number during adolescent growth could take place in the absence of myocyte death or could occur in addition to ongoing myocyte turnover. A significant number of TUNEL⁺ myocyte nuclei were observed in both 11- and 22-week animals, with no significant differences found at these ages (11 weeks versus 22 weeks: 0.083±0.015% versus 0.077±0.017% TUNEL⁺ myocyte nuclei). These findings suggest that to increase myocyte number during adolescent growth, new myocyte formation must be in excess of the rate of myocyte apoptosis.

SMMs Contract Slower and Relax Slower Than LBM

Contractions (Figure 4A) in SMMs (7.6±0.6%) and LBMs (8.1±0.9%) were not significantly different (Figure 4B). However, the maximum shortening and relaxation rates were significantly slower in SMMs (Figure 4C). The times to 50% shortening, to peak shortening, and to 50% relaxation were all significantly longer in SMMs (Figure 4D).

Ca²⁺ Transients in SMMs Have Two Phases and Are Slowly Rising

The peak amplitude of the Ca²⁺ transient in SMMs was significantly lower than in LBMs (1.83±0.11, n=26, N=6 versus 2.29±0.16, n=25, N=6, respectively, P<0.05; Figure 5A and 5B). The time to peak Ca²⁺ in SMMs was significantly longer than in LBMs (165.9±14.2/ms, n=26, N=6 versus 101.1±14.2/ms, n=25, N=5, P<0.01) and the maximal rate of rise of the Ca²⁺ transient was significantly slower in SMMs versus in LBMs ([F/F₀]/ms: 0.122±0.019/ms versus 0.057±0.011/ms) (Figure 5D and 5E). The rising phase of the Ca²⁺ transient in SMMs had an initial rapidly rising phase and a secondary, slower, rising phase. There was primarily a rapidly rising portion in LBMs (Figure 5A and 5C). The configuration of the Ca²⁺ transient in SMMs is similar to the type reported in neonatal myocytes.² The duration of the fast rising phase (SMMs versus LBMs: 29.8±2.0 ms, n=26, N=6 versus 44.8±6.9ms, n=25, N=5, P<0.05) was significantly shorter and the contribution of the rapidly rising phase to the total amplitude (SMMs versus LBMs: 71.9±4.7%, n=26, N=6 versus 92.2±2.5%, n=25, N=5, P<0.05) was significantly smaller in SMMs (Figure 5E). The time between the peak of the rapidly rising phase and the peak of the slowly rising phase was significantly longer (P<0.01) in SMMs (136.1±1.7ms, n=26, N=6) than in LBMs (56.1±0.8 ms, n=25, N=5).

The decay of the Ca²⁺ transient also has 2 portions that could be fit with a monoexponential function.¹⁷ The time constant of the initial decay period was significantly slower in SMMs than in LBMs (248.2±25.0 ms, n=26, N=6 versus 180.1±17.9 ms, n=25, N=6, P<0.001; Figure 5F). These

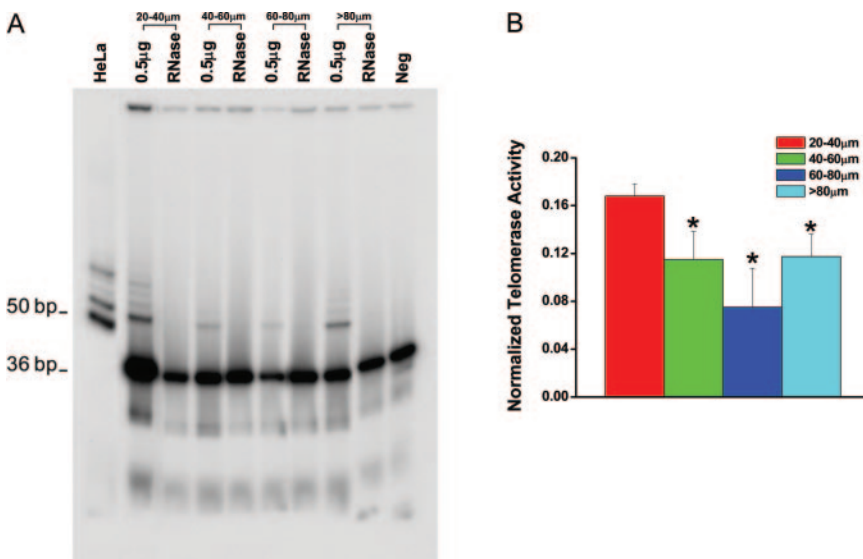


Figure 3. Telomerase activity is greater in small VMs. A, Representative example of telomerase activity in feline myocytes separated by filter size (20 to >80 μm) using the telomeric repeat amplification protocol (TRAP); 0.5 of cell extract per lane. Products of telomerase activity start at 50 bp and display 6-bp periodicity. Myocyte extracts treated with RNase were used as negative controls and HeLa cell extract as positive control. Neg indicates having lysis buffer only. B, Normalized telomerase activity was highest in small VMs (20 to 40 μm). *P<0.05 vs VMs in 20- to 40-μm fraction when 0.5 μg of VM extract was used.

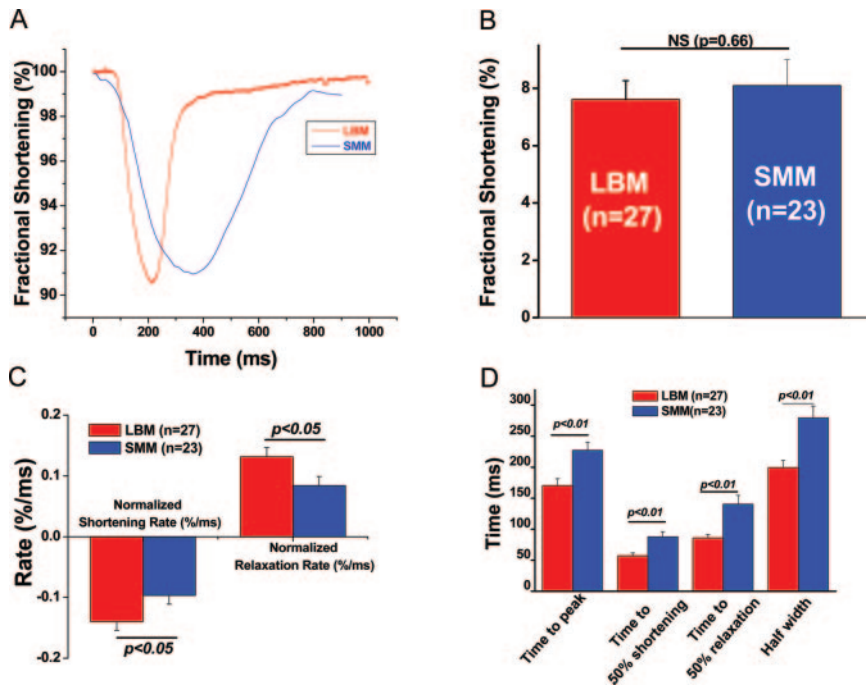


Figure 4. Contractions in SMMs are slower and longer than in LBMs. A, Representative examples of contractions of a SMM and an LBM. B, Fractional shortening was not different in SMMs vs LBMs. C and D, The rates of contraction and relaxation of SMMs were significantly slower than in LBMs.

results indicate that the excitation/contraction (EC) coupling machinery (the T-tubular system and the SR) is not fully developed in SMMs.

Ca²⁺ Release During the Early Phase of the Ca²⁺ Transient Is Less Synchronized in SMMs

Ca²⁺ release is less well spatially synchronized within fetal and neonatal than in adult ventricular myocytes.¹⁸ This is primarily attributable to a more rudimentary T-tubule/sarcoplasmic reticulum (SR) coupling, which is essential for normal EC coupling in the adult heart.¹⁸ We explored the idea that a less well organized T-tubular system is responsible for a less well organized SR Ca²⁺ release in SMMs by measuring Ca²⁺ transients with confocal microscopy (line-scan imaging) in myocytes paced at 0.5 Hz. SR Ca²⁺ release was spatially less well organized in SMMs, revealed by the uneven wave front of their Ca²⁺ transients (Figure 5G and 5H). The synchrony of Ca²⁺ release, assessed by the percentage of pixels with intensity over half maximum intensity (%F>F50),¹⁶ was significantly smaller in SMMs than LBMs (Figure 5I). These results suggest that components necessary for the synchronized SR Ca²⁺ release of normal adult cardiac myocytes are not fully developed in SMMs.

Two processes that could produce this less synchronized SR Ca²⁺ release are a less well organized T-tubular system (the absence of some release sites) and/or electrophysiological differences that would cause a fraction of release sites to fail to release their stored Ca²⁺.¹⁶ A decrease in the density of the transient outward potassium current (*I_{to}*) elevates the early portion of the cardiac action potential and reduces Ca²⁺ entry through the L-type calcium channel.¹⁶ We have previously shown that in hypertrophied ventricular myocytes, this can cause dyssynchronous SR Ca²⁺ release.¹⁶ There were no significant differences in resting membrane potentials, phase 0 maximum rising rates, peak or plateau voltages, or the

duration of the action potentials (APs) between SMMs and LBMs (Figure 6A). However, there were significant differences in the early and late AP repolarization phases, which are largely dictated by K⁺ currents.¹⁹ Phase 1 repolarization was significantly less prominent in SMMs (15.3±2.1 mV, n=18, N=5) than in LBMs (22.2±2.5 mV, n=18, N=5, P<0.05) and the maximum repolarization rate of phase 3 was significantly slower in SMMs (-1.29±0.18 mV/ms, n=18 versus -1.87±0.22 mV/ms in n=18 LBMs, P<0.05). The 4-aminopyridine-sensitive, transient outward current (*I_{to}*) that controls phase 1 repolarization¹⁶ was smaller in SMMs than in LBMs (Figure 6D through 6F). The T-tubule density (T-tubular index, as described by He et al¹⁴) in 1-(3-sulfonatopropyl)-4-[β[2-(di-n-octylamino)-6-naphthyl]vinyl]pyridinium betaine (Di-8-ANEPPS)-labeled myocytes (Figure 6G through 6I) was significantly smaller in SMMs (15.1±1.4% versus 24.3±1.5% in LBMs, P<0.01). These differences in T-tubule and *I_{to}* density should contribute to the spatial disorganization of Ca²⁺ release^{2,16} observed in SMMs.

SMMs Have T-type Calcium Current

The functional roles of TTCC currents (*I_{Ca-T}*) in adult VMs are still not fully understood. *I_{Ca-T}* is present in embryonic and neonatal VMs but not in most adult VMs, implying a developmental role for Ca²⁺ flux through this channel.⁶ We showed many years ago that pressure overload induces a "reexpression" of T-type Ca²⁺ channels in adult feline VMs.²⁰ A number of related studies in noncardiac cells have shown that the T-type calcium channel plays an important role in differentiation, growth, and proliferation.⁶ We suggest that the TTCC may have a role in the generation of new cardiac myocytes and/or in the maturation of newly formed into fully functional VMs. As a first test of these ideas, we measured *I_{Ca-T}* and *I_{Ca-L}* (L-type calcium current, the major Ca²⁺ channel current in cardiac myocytes) in SMMs and LBMs (Figure 7A

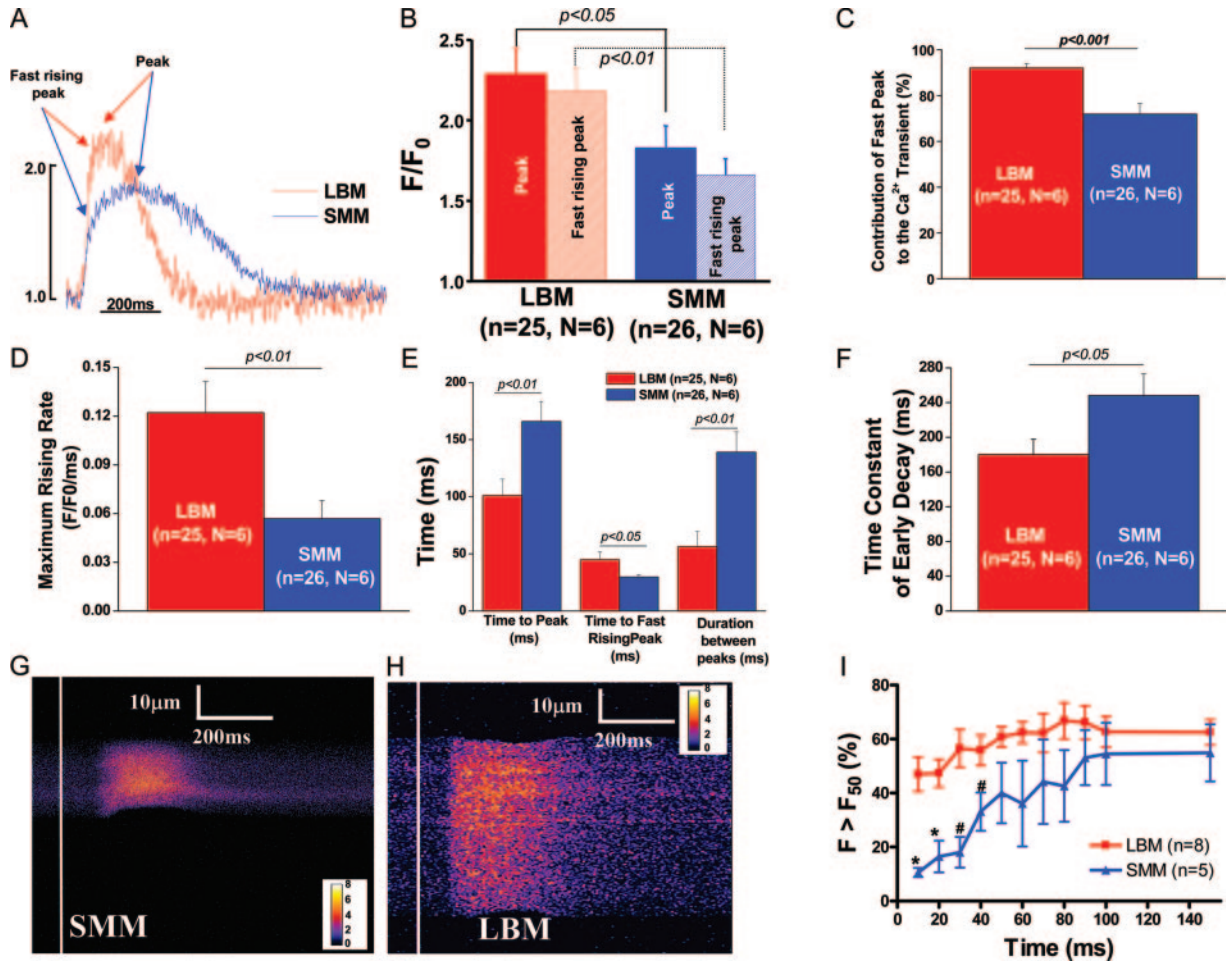


Figure 5. Ca²⁺ transient in SMMs are smaller and reach their peak more slowly than in LBMs. A, Ca²⁺ transient in SMMs had rapid and then slow rising phases, which were not apparent in LBMs. B, The peak of Ca²⁺ transient and the amplitude of the rapidly rising phase in SMMs were significantly lower in SMMs. C, The contribution of the rapidly rising phase to the Ca²⁺ transient was smaller in SMMs. D, The maximum rate of rise was slower in SMMs. E, The time to peak, the time between the peak of the rapidly rising phase, and the peak of the slowly rising phase was significantly prolonged in SMMs. F, The decay of the Ca²⁺ transient was divided into initial and terminal portions. The time constant of the initial decay period was significantly longer in SMMs than in LBMs. G and I, Confocal line-scan imaging shows that Ca²⁺ release in SMMs is disorganized (G) during the first 40 ms (I) of the Ca²⁺ transient. Lines in G and H (a 4-ms flash) are 90 ms before of the stimuli. **P*<0.01 in SMMs vs in LBMs, #*P*<0.05 in SMMs vs in LBMs.

and 7B) using established techniques based on differences in their voltage dependence of activation and inactivation⁶ (Figure 7D, 7E, and 7G). *I*_{Ca-T} (-3.0±0.6 pA/pF) was found in 11 of 19 SMMs (57.6±4.0 pF). No detectable *I*_{Ca-T} was found in any of the 18 LBMs (139.9±9.6 pF) examined, similar to what we have reported previously.²⁰ *I*_{Ca-L} was present in all myocytes and its density was not different in SMMs and LBMs (Figure 7D and 7E). *I*_{Ca-T} (and *I*_{Ca-L}) was also observed in 3 myocytes derived from cardiac c-Kit⁺ stem cells maintained in coculture with neonatal rat cardiomyocytes (Figure 7C and 7F). The T-type Ca²⁺ current in the SMMs and cKit⁺ CS/PC-derived myocytes likely reflects Ca²⁺ influx through the α_{1H} TTCC gene, because these currents were blocked by low concentrations of Ni²⁺ and were insensitive to Cd²⁺ (Figure 7H and 7I).²¹ These studies support an association between Ca²⁺ influx through the TTCC and new myocyte generation.

Discussion

The present study was performed in adolescent animals undergoing a rapid growth phase, near the time of sexual

maturity, because it was our view that if new myocyte formation were part of the normal physiology of the postnatal heart, then the capacity to generate these new myocytes should be evident during this period of robust physiological cardiac growth. Our results show that (1) the increase in the size of the adolescent heart is greater than the enlargement of its individual myocytes, supporting myocyte hyperplasia above and beyond the rate of myocyte apoptosis; (2) the young adult heart has a population of small mononucleated ventricular myocytes that are BrdUrd⁺, Ki67⁺, P16^{INK4a+} and have telomerase activity; and (3) SMMs have physiological properties reminiscent of fetal/neonatal myocyte.

What Is the Source of Newly Formed Ventricular Myocytes?

Although we clearly show that new myocytes are small and mononucleated with immature functional properties that are reminiscent of fetal/neonatal myocytes,² we cannot discriminate between CS/PCs and small proliferative myocytes as the source of the new myocytes in the adolescent heart. The

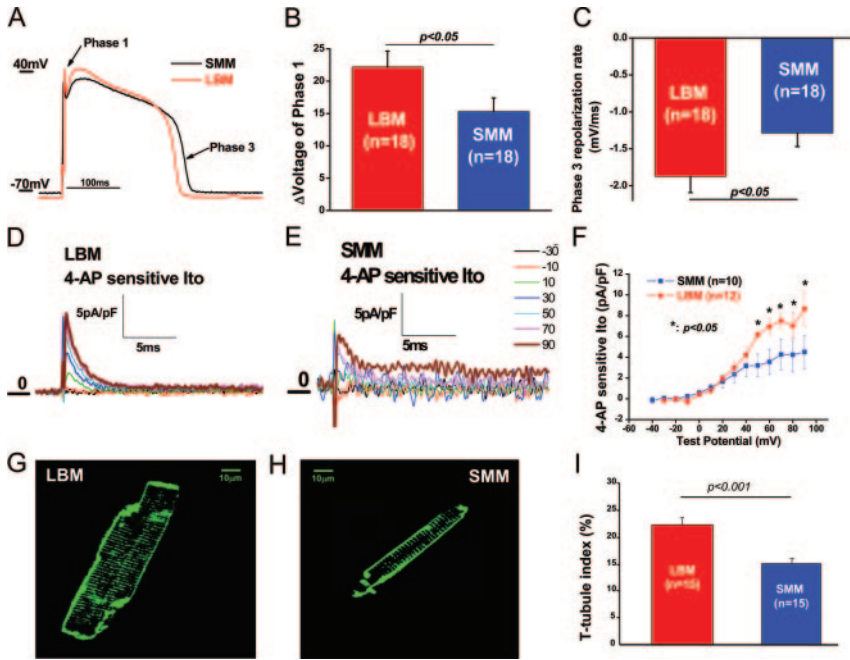


Figure 6. SMMs have less I_{to} and T-tubule density than LBMs. A, AP configuration was similar in SMMs and LBM. However, The voltage change during phase 1 repolarization was significantly smaller (A and B) and the maximum repolarization rate of phase 3 was significantly slower (A and C) in SMMs than in LBMs. D through F, 4-Aminopyridine (4-AP) sensitive current (I_{to}) was smaller in SMMs than in LBMs. Di-8-ANEPPS-stained SMMs and LBMs are shown in G and H. I, T-Tubule index in SMMs was less than in LBMs.

recognition that telomerase activity is present in small cycling myocytes is consistent with the notion that these dividing cells represent a population of amplifying myocytes derived from a primitive pool of c-kit⁺ CS/PCs. Our in vitro studies have shown that this class of undifferentiated progenitor cells can acquire the cardiomyogenic fate leading to the generation of functionally competent myocytes.¹ Together, these results indicate that the adolescent feline heart retains a remarkable degree of developmental plasticity with the inherent ability to create a significant number of new myocytes to accommodate its increasing hemodynamic demands.

A number of laboratories have identified populations of resident CS/PCs that have the capacity to differentiate into new cardiac myocytes both in vitro and in vivo.^{1,22-24} These

include cells expressing the receptor tyrosine kinase c-Kit,¹ stem cell antigen-1 (Sca-1),²³ side population (SP) cells that can exclude the DNA-binding dye Hoechst 33258, and even cells expressing the transcription factor isl-1.²² The role of each of these cell types in the generation of new myocytes in the adolescent heart is yet to be determined.

SMMs Have Immature Functional Properties

In a previous study, we tested the idea that cardiac contractility varied with cell size in both the normal and hypertrophied (pressure overload) heart.²⁵ This study clearly showed that myocytes from hypertrophied hearts were functionally distinct from those in the normal heart, but, in neither the normal or hypertrophied hearts, was myocyte function related

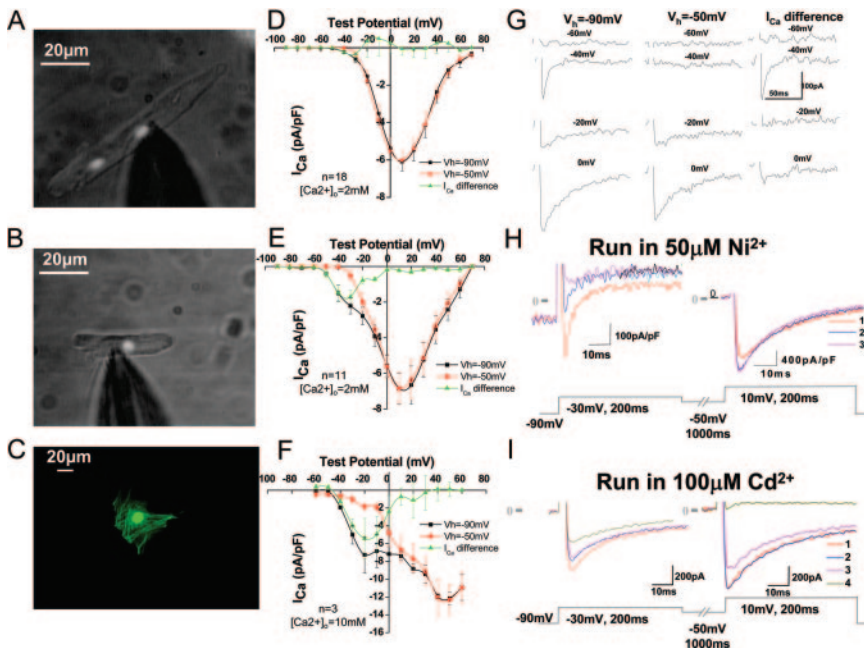


Figure 7. I_{Ca-T} is present in SMMs but not in LBMs. Representative SMMs (A), LBMs (B), and cKit⁺ CS/PC-derived myocytes (C) used for electrophysiological measurements are shown. Average data of Ca^{2+} current recordings at the holding potentials of -90 and -50 mV and the differences (I_{Ca-T}) in these cells are shown in D through F. Representative raw data from a SMM is shown in G. The current peaked around -30 mV (I_{Ca-T}) was blocked by $50 \mu\text{mol/L Ni}^{2+}$ (H) but was insensitive to Cd^{2+} (I).

to myocyte size. Although a broad range of myocyte sizes were examined, the smallest myocytes from both the normal and hypertrophied hearts were not studied. We characterized the physiological properties of SMMs for the first time and determined that they are functionally immature and distinct from the LBMs, which make up the majority of the young adult heart.

The functional properties of cardiac myocytes derived from embryonic stem cells (ESCs),²⁶ hematopoietic stem cells,²⁷ and cardiac stem cells (CSCs) in culture are also functionally immature. In cardiac myocytes derived from ESCs,²⁸ the transient outward K^+ and L-type Ca^{2+} currents are expressed first, followed by cardiac-specific Na^+ current, the delayed rectifier K^+ current, and I_f currents, and, in the latest stages, inwardly rectifying K^+ and ATP-sensitive K^+ currents are observed. These changes in ion channel expression are similar to those seen during the development of cardiac myocytes in vivo and resemble those of cardiac myocytes in embryonic heart tubes.²⁹ Matsuura et al³⁰ reported that oxytocin induces Sca-1⁺ CSCs from the adult murine heart to differentiate into functional, spontaneously beating, immature cardiomyocytes with Ca^{2+} transients. These cells had positive inotropic responses to isoproterenol via β_1 -adrenergic receptor signaling. ESC-derived cardiac myocytes also responded to isoproterenol and carbachol.³¹ Collectively, these studies show that ESCs and CS/PC-derived cardiac myocytes express the ion channels seen in the developing, but immature heart.

SMMs Express TTCCs

The present experiments show that SMMs with immature functional properties express TTCCs. Because the TTCC is not an effective inducer of SR Ca^{2+} release,³² the functional significance of Ca^{2+} influx through the TTCC in VMs is, in our view, still not known. The TTCC is present in fetal/neonatal ventricular myocytes,³³ in cardiac myocytes derived from mouse embryonic stem cells,³⁴ but not in most adult ventricular myocytes,³³ suggestive of some developmental function.³⁵ The disappearance of T-type calcium current (I_{Ca-T}) after birth parallels the withdrawal of VMs from the cell cycle,⁶ suggesting it may have some role in cell cycle regulation. We previously showed that I_{Ca-T} reemerges in adult feline VMs under pathological cardiovascular stress,²⁰ which we proposed was related to induction of a fetal gene program. We now hypothesize that the presence of TTCCs in SMMs is associated with the fact that these VMs were recently formed. These ideas are supported by studies in other cell types (see below) but need to be examined in detail in cardiac myocytes.

Ca^{2+} influx through the TTCC plays a critical role in the proliferation of blastocyte-derived embryonic stem cells, fibroblasts, vascular smooth muscle,⁶ and even neonatal ventricular myocytes.³³ Blockade of I_{Ca-T} inhibits proliferation of smooth muscle as well as differentiation of neuronal stem cells.⁶ We speculate that TTCCs play an important signaling function during the generation of newly formed ventricular myocytes in the adolescent heart. Whether TTCCs are expressed on CSCs during their conversion to the myocyte lineage and their subsequent maturation are important un-

answered questions. Because TTCCs appear to modulate the growth and differentiation of smooth muscle and endothelial cells,⁶ they may be a key regulator of the commitment of multipotent CS/PCs to the various cardiac cell classes.

Limitations

Many of the critical experiments in this study used isolated myocytes, with the assumption that we isolated myocytes that were representative of the entire heart. Although we think the possibility is unlikely, there would be bias in the cell volume calculations if selective subpopulations of myocytes were not routinely isolated.

Clinical Implications

The generation of new myocytes is potentially a groundbreaking therapy for the treatment of cardiac diseases, especially those that involve a critical reduction in the number of cardiac myocytes, such as myocardial infarction and congestive heart failure.¹ A number of recent studies in human patients and in animal models¹ suggest that delivery of exogenous stem cells to the damaged heart leads to improved cardiac function. Although the mechanism by which nonresident progenitor cells results in improved function remains unclear,¹ our findings point to the role that resident progenitor cells and their early committed progeny may have in cardiac growth and repair.¹ The generation of new myocytes in the young heart is a normal physiological process and if confirmed later in life would strongly suggest that the understanding of the regulatory mechanisms of myocyte formation in the adult organ may be of fundamental biological importance and could have significant translational impact on patients with debilitating cardiac disorders.

Sources of Funding

Supported by NIH RO1 grants HL61495 and HL33921.

Disclosures

None.

References

1. Leri A, Kajstura J, Anversa P. Cardiac stem cells and mechanisms of myocardial regeneration. *Physiol Rev*. 2005;85:1373–1416.
2. Haddock PS, Coetzee WA, Cho E, Porter L, Katoh H, Bers DM, Jafri MS, Artman M. Subcellular $[Ca^{2+}]_i$ gradients during excitation-contraction coupling in newborn rabbit ventricular myocytes. *Circ Res*. 1999;85:415–427.
3. Soonpaa MH, Field LJ. Survey of studies examining mammalian cardiomyocyte DNA synthesis. *Circ Res*. 1998;83:15–26.
4. MacLellan WR, Schneider MD. Genetic dissection of cardiac growth control pathways. *Annu Rev Physiol*. 2000;62:289–319.
5. Chimenti C, Kajstura J, Torella D, Urbanek K, Heleniak H, Colussi C, Di Meglio F, Nadal-Ginard B, Frustaci A, Leri A, Maseri A, Anversa P. Senescence and death of primitive cells and myocytes lead to premature cardiac aging and heart failure. *Circ Res*. 2003;93:604–613.
6. Yunker AM, McEnery MW. Low-voltage-activated (“T-Type”) calcium channels in review. *J Bioenerg Biomembr*. 2003;35:533–575.
7. Rodman DM, Reese K, Harral J, Fouty B, Wu S, West J, Hoedt-Miller M, Tada Y, Li KX, Cool C, Fagan K, Cribbs L. Low-voltage-activated (T-type) calcium channels control proliferation of human pulmonary artery myocytes. *Circ Res*. 2005;96:864–872.
8. Bailey BA, Houser SR. Sarcoplasmic reticulum-related changes in cytosolic calcium in pressure-overload-induced feline LV hypertrophy. *Am J Physiol*. 1993;265(6 pt 2):H2009–H2016.
9. Beltrami AP, Barlucchi L, Torella D, Baker M, Limana F, Chimenti S, Kasahara H, Rota M, Musso E, Urbanek K, Leri A, Kajstura J, Nadal-

- Ginard B, Anversa P. Adult cardiac stem cells are multipotent and support myocardial regeneration. *Cell*. 2003;114:763–776.
10. Kajstura J, Mansukhani M, Cheng W, Reiss K, Krajewski S, Reed JC, Quaini F, Sonnenblick EH, Anversa P. Programmed cell death and expression of the protooncogene bcl-2 in myocytes during postnatal maturation of the heart. *Exp Cell Res*. 1995;219:110–121.
 11. Gerdes AM, Kriseman J, Bishop SP. Changes in myocardial cell size and number during the development and reversal of hyperthyroidism in neonatal rats. *Lab Invest*. 1983;48:598–602.
 12. Kajstura J, Zhang X, Liu Y, Szoke E, Cheng W, Olivetti G, Hintze TH, Anversa P. The cellular basis of pacing-induced dilated cardiomyopathy. Myocyte cell loss and myocyte cellular reactive hypertrophy. *Circulation*. 1995;92:2306–2317.
 13. Leri A, Barlucchi L, Limana F, Deptala A, Darzynkiewicz Z, Hintze TH, Kajstura J, Nadal-Ginard B, Anversa P. Telomerase expression and activity are coupled with myocyte proliferation and preservation of telomeric length in the failing heart. *Proc Natl Acad Sci U S A*. 2001;98:8626–8631.
 14. He J, Conklin MW, Foell JD, Wolff MR, Haworth RA, Coronado R, Kamp TJ. Reduction in density of transverse tubules and L-type Ca(2+) channels in canine tachycardia-induced heart failure. *Cardiovasc Res*. 2001;49:298–307.
 15. Chen X, Zhang X, Kubo H, Harris DM, Mills GD, Moyer J, Berretta R, Potts ST, Marsh JD, Houser SR. Ca²⁺ influx-induced sarcoplasmic reticulum Ca²⁺ overload causes mitochondrial-dependent apoptosis in ventricular myocytes. *Circ Res*. 2005;97:1009–1017.
 16. Harris DM, Mills GD, Chen X, Kubo H, Berretta RM, Votaw VS, Santana LF, Houser SR. Alterations in early action potential repolarization causes localized failure of sarcoplasmic reticulum Ca²⁺ release. *Circ Res*. 2005;96:543–550.
 17. Chaudhary KW, Rossman EI, Piacentino V, 3rd, Kenessey A, Weber C, Gaughan JP, Ojamaa K, Klein I, Bers DM, Houser SR, Margulies KB. Altered myocardial Ca²⁺ cycling after left ventricular assist device support in the failing human heart. *J Am Coll Cardiol*. 2004;44:837–845.
 18. Seki S, Nagashima M, Yamada Y, Tsutsuura M, Kobayashi T, Namiki A, Tohse N. Fetal and postnatal development of Ca²⁺ transients and Ca²⁺ sparks in rat cardiomyocytes. *Cardiovasc Res*. 2003;58:535–548.
 19. Tamargo J, Caballero R, Gomez R, Valenzuela C, Delpon E. Pharmacology of cardiac potassium channels. *Cardiovasc Res*. 2004;62:9–33.
 20. Nuss HB, Houser SR. T-type Ca²⁺ current is expressed in hypertrophied adult feline left ventricular myocytes. *Circ Res*. 1993;73:777–782.
 21. Lee JH, Gomora JC, Cribbs LL, Perez-Reyes E. Nickel block of three cloned T-type calcium channels: low concentrations selectively block alpha1H. *Biophys J*. 1999;77:3034–3042.
 22. Laugwitz KL, Moretti A, Lam J, Gruber P, Chen Y, Woodard S, Lin LZ, Cai CL, Lu MM, Reth M, Platoshyn O, Yuan JX, Evans S, Chien KR. Postnatal is11+ cardioblasts enter fully differentiated cardiomyocyte lineages. *Nature*. 2005;433:647–653.
 23. Oh H, Bradfute SB, Gallardo TD, Nakamura T, Gaussin V, Mishina Y, Pocius J, Michael LH, Behringer RR, Garry DJ, Entman ML, Schneider MD. Cardiac progenitor cells from adult myocardium: homing, differentiation, and fusion after infarction. *Proc Natl Acad Sci U S A*. 2003;100:12313–12318.
 24. Pfister O, Mouquet F, Jain M, Summer R, Helmes M, Fine A, Colucci WS, Liao R. CD31- but Not CD31+ cardiac side population cells exhibit functional cardiomyogenic differentiation. *Circ Res*. 2005;97:52–61.
 25. Duthinh V, Houser SR. Contractile properties of single isolated feline ventricular myocytes. *Am J Physiol*. 1988;254(1 pt 2):H59–H66.
 26. He JQ, Ma Y, Lee Y, Thomson JA, Kamp TJ. Human embryonic stem cells develop into multiple types of cardiac myocytes: action potential characterization. *Circ Res*. 2003;93:32–39.
 27. Xu W, Zhang X, Qian H, Zhu W, Sun X, Hu J, Zhou H, Chen Y. Mesenchymal stem cells from adult human bone marrow differentiate into a cardiomyocyte phenotype in vitro. *Exp Biol Med (Maywood)*. 2004;229:623–631.
 28. Maltsev VA, Wobus AM, Rohwedel J, Bader M, Hescheler J. Cardiomyocytes differentiated in vitro from embryonic stem cells developmentally express cardiac-specific genes and ionic currents. *Circ Res*. 1994;75:233–244.
 29. Fijnvandraat AC, van Ginneken AC, de Boer PA, Ruijter JM, Christoffels VM, Moorman AF, Lekanne Deprez RH. Cardiomyocytes derived from embryonic stem cells resemble cardiomyocytes of the embryonic heart tube. *Cardiovasc Res*. 2003;58:399–409.
 30. Matsuura K, Nagai T, Nishigaki N, Oyama T, Nishi J, Wada H, Sano M, Toko H, Akazawa H, Sato T, Nakaya H, Kasanuki H, Komuro I. Adult cardiac Sca-1-positive cells differentiate into beating cardiomyocytes. *J Biol Chem*. 2004;279:11384–11391.
 31. Reppel M, Boettinger C, Hescheler J. Beta-adrenergic and muscarinic modulation of human embryonic stem cell-derived cardiomyocytes. *Cell Physiol Biochem*. 2004;14:187–196.
 32. Sipido KR, Carmeliet E, Van de Werf F. T-type Ca²⁺ current as a trigger for Ca²⁺ release from the sarcoplasmic reticulum in guinea-pig ventricular myocytes. *J Physiol*. 1998;508(pt 2):439–451.
 33. Guo W, Kamiya K, Kodama I, Toyama J. Cell cycle-related changes in the voltage-gated Ca²⁺ currents in cultured newborn rat ventricular myocytes. *J Mol Cell Cardiol*. 1998;30:1095–1103.
 34. Zhang YM, Shang L, Hartzell C, Narlow M, Cribbs L, Dudley SC Jr. Characterization and regulation of T-type Ca²⁺ channels in embryonic stem cell-derived cardiomyocytes. *Am J Physiol Heart Circ Physiol*. 2003;285:H2770–H2779.
 35. Wetzel GT, Klitzner TS. Developmental cardiac electrophysiology recent advances in cellular physiology. *Cardiovasc Res*. 1996;31:E52–E60.

Materials and Methods

BrdU infusion into normal cats: Osmotic pumps (ALZET) were filled with 50mg/mL BrdU dissolved in 50% DMSO/50% ddH₂O filtered through a sterile 0.22µm filter. Pumps were then incubated in sterile saline at 37 °C overnight prior to insertion. The pumps were surgically inserted subcutaneously just caudal to the scapulae per the protocol approved by IACUC at Temple University. The number of pumps was varied depending on animal body weight for an average infusion of 10mg/kg/day for seven days.

Myocyte and CSC isolation: Ventricular myocytes (Ms)^{1,2} and cardiac stem/progenitor cells (CS/PCs)³ were isolated from adolescent feline hearts. Initial yields from the cell isolation are consistently 80-90% rod-shaped myocytes. The supernatant obtained after allowing the myocytes to gravity settle was used for isolating CSCs. For immunostaining and biochemical studies, ventricular myocytes from the left ventricle (including free wall and septum) were used. Samples were divided into septum and LV free wall, but identical results were obtained and data were combined. The techniques used produced a high % (>80%) of rod shaped ventricular myocytes. For electrophysiological measurements, only myocytes from left ventricular free wall were used. These myocytes were maintained at room temperature with a 5% CO₂, and 95% O₂ overlay and used within 12 hours of isolation. To isolate CSCs, cells in the supernatant were incubated with an antibody against c-Kit (Santa Cruz) and c-Kit positive CSCs were separated and purified with magnetic beads (Miltenyi Biotech) coated with an anti-IgG antibody. The purity of the sorted cells was assessed by FACS or immunocytochemistry with antibody against c-Kit.

Co-culture of rat neonatal ventricular myocytes and GFP-labeled feline c-Kit⁺ cells:

Neonatal rat ventricular myocytes were isolated and cultured as described previously⁴. Isolated CSCs were cultured in medium DMEM containing 5% FBS, 20U/L insulin and transferrin and transfected with an adenovirus containing an enhanced GFP (AdGFP) gene at the MOI of 50 for 2 days. Transfected CSCs were then washed with a medium DMEM followed by dissociation with Trypsin-EDTA (Sigma). CSCs were added to the culture dish with neonatal VMs and co-cultured for 2-3 days. CSC-derived new myocytes that were spontaneously beating and had GFP expression were selected for Ca²⁺ current measurement. CSCs in co-culture for 2 days were fixed so that we could measure the % of CSC-derived cells (GFP expressing) that were expressing cardiac contractile proteins and had organized sarcomeres. These measurements were made in at least 100 cells from 4 separate preparations, and 212 of 414 CSC-derived cells were found to have organized sarcomeres.

Immunostaining for BrdU and Ki67 in cardiac myocytes and myocyte size

measurements: Cells were isolated, washed and plated on laminin-coated, positively charged slides in M199 culture medium (Sigma, St. Louis, MO) with penicillin G (100000u/L), streptomycin (100mg/L), and gentamycin (50mg/L) for 1 hour. For BrdU staining, the protocol was modified from protocol from Roche BrdU Labeling and Detection Kit 1 (Roche Applied Sciences, Indianapolis, IN). In brief, slides were fixed in 70% ethanol with 15mM glycine, pH 2.0 adjusted with HCl, for 30 minutes at -20 °C. The fixative solution was replaced with fresh fixative and incubated overnight at -20 °C. Slides were washed with phosphate buffered saline (PBS, in mM: NaCl 136.9, KCl 2.68,

Na₂HPO₄ 10.1, NaH₂PO₄ 2.0) and incubated in PBS at 37 °C for 30 minutes to fully rehydrate cells. Anti-BrdU antibody (in incubation buffer containing nucleases to allow access of the antibody to the BrdU) was added and incubated at 37 °C for 90 minutes. Slides were washed with PBS, then the secondary antibody tagged with fluorescein was added and incubated at 37 °C for 90 minutes. 4',6-diamidino-2-phenylindole (DAPI, Molecular Probes, Carlsbad CA) was added for 5 minutes at the end of the secondary incubation. Slides were washed with PBS, then covered with mounting medium (Vectashield, Vector Laboratories, Burlingame CA) and coverslips. For Ki67 staining, slides were fixed with ice-cold methanol for 10 minutes at -20 °C, then washed with PBS. Primary antibody (rabbit polyclonal anti-Ki67, Vector Labs, Burlingame CA) was added and slides were incubated 90 min at 37 °C. Slides were washed with PBS and incubated overnight at 4 °C with a rhodamine secondary (donkey anti-rabbit, Jackson Labs). DAPI and mounting medium was added as for the BrdU labeling. Slides were analyzed with fluorescence microscopy. The percentages of mononucleated, binucleated and multinucleated myocytes as well as the percentage of BrdU and Ki67 positive nuclei were measured. Images of stained cells and a micrometer were acquired with an Olympus fluorescence microscope and two dimensional sizes were analyzed for mono- and binucleated myocytes with the Scion Image software (NIH). Cell depth was measured with the aid of confocal microscopy (Nikon) for calculating cell volume as described previously⁵. Our preliminary studies showed that all isolated myocytes including large binucleated and small mononucleated myocytes were c-Kit⁻, Scal⁻ and CD31⁻. Hence these small mononucleated myocytes are different from the cells studied by Wang et al⁶.

Separation of small and large myocytes: Freshly isolated VMs were separated by filtration through nylon meshes (BD Biosciences and Spectrum Laboratories Inc.) with pore sizes of 20, 40, 60 and 80 μ m. VMs not passing the 80 μ m-mesh were washed off with medium 199 and considered as > 80 μ m. Cells passing the 80 μ m-mesh were further filtered by a 60 μ m-mesh. VMs not passing the 60 μ m-mesh were washed off and considered as 60-80 μ m. By this way, we separated myocytes into 4 fractions (20-40 μ m, 40-60 μ m, 60-80 μ m and >80 μ m) and telomerase activity in each fraction was measured as described below.

Telomeric Repeat Amplification Protocol (TRAP): Myocytes were homogenized in 3-[(3-cholamidopropyl)dimethyl-ammonio]-1-propanesulfonate (CHAPS) buffer, kept on ice for 30 minutes and centrifuged for 20 minutes at 4°C. For each fraction of VMs, 0.5 and 1.0 μ g of untreated and RNase-treated myocyte extracts were incubated with 0.1 μ g of [γ -³²P]ATP end-labeled telomerase substrate (TS oligonucleotide: 5'-AAT CCG TCG AGC AGA GTT-3') for 30 minutes in the following solution: 20mM Tris-HCl, 1.5mM MgCl₂, 68mM KCl, 1mM EGTA, 0.05% Tween 20, 50mM dNTPs, 2 U of Taq DNA polymerase, 0.1 μ g of anchored reverse primer (5'-GCG CGC [CTT ACC]₃ CTA ACC-3'), pH 8.3. Samples were exposed to 31 amplification cycles of 94°C for 30 seconds, 50°C for 30 seconds and 72°C for 3 minutes. Polymerase chain reaction (PCR) products were separated on 12% polyacrylamide gel. Each reaction mixture contained two oligonucleotides, K1 and TSK1, which, together with TS, produced in each lane a 36-bp band. This band was utilized as internal control for the efficiency of the PCR. Additionally, HeLa cell extracts (0.5 and 1 μ g), were used as a positive control. The

telomerase-induced reaction generated a 6-bp ladder. The optical density (OD) of the bands was measured to evaluate telomerase activity; the gel lane signal corresponding to the ladder bands was normalized for PCR efficiency and compared with that obtained by 1 attomol of TSR8. TSR8 is an oligonucleotide identical to TS with the addition of eight telomeric repeats.

Functional measurements in small mononucleated and large binucleated myocytes:

Isolated VMs were stained with 1 μ g/ml Hoechst 33258 for 15 minutes and then the dye was washed off. VMs were placed in a chamber mounted on an inverted Nikon microscope and perfused with normal physiological solution (Tyrode) containing 1mM Ca²⁺. SMMs and LBMs were selected to measure contractions with video edge detector. Simultaneously intracellular Ca²⁺ was measured with PMT collecting the emission (520nm) from Fluo-4 excited at 488nm. Action potentials, whole-cell calcium ([Ca²⁺]_o=2mM) and transient outward currents ([K⁺]_i=140mM, [K⁺]_o=10mM) were recorded as describe previously⁷⁻⁹. Perforated patch technique was used for AP studies. Confocal line scanning was used to reveal the synchrony of Ca²⁺ release¹⁰.

Statistics: Descriptive statistics (mean, median, standard deviation, standard error of the mean (SEM)) were calculated for each parameter measured. Proper comparison statistics (t-test, ANOVA or Fisher's exact test) were used to compare parameters measured in different groups of cells at the significance level of 0.05. The occurrence of the characteristics of interest (mono-, bi-nucleation, t-type calcium current, etc.) was compared between size categories.

References Cited

1. Silver LH, Hemwall EL, Marino TA, Houser SR. Isolation and morphology of calcium-tolerant feline ventricular myocytes. *Am J Physiol.* 1983;245:H891-896.
2. Bailey BA, Houser SR. Sarcoplasmic reticulum-related changes in cytosolic calcium in pressure-overload-induced feline LV hypertrophy. *Am J Physiol.* 1993;265:H2009-2016.
3. Beltrami AP, Barlucchi L, Torella D, Baker M, Limana F, Chimenti S, Kasahara H, Rota M, Musso E, Urbanek K, Leri A, Kajstura J, Nadal-Ginard B, Anversa P. Adult cardiac stem cells are multipotent and support myocardial regeneration. *Cell.* 2003;114:763-776.
4. Gaughan JP, Hefner CA, Houser SR. Electrophysiological properties of neonatal rat ventricular myocytes with alpha1-adrenergic-induced hypertrophy. *Am J Physiol.* 1998;275:H577-590.
5. Kajstura J, Zhang X, Liu Y, Szoke E, Cheng W, Olivetti G, Hintze TH, Anversa P. The cellular basis of pacing-induced dilated cardiomyopathy. Myocyte cell loss and myocyte cellular reactive hypertrophy. *Circulation.* 1995;92:2306-2317.
6. Wang X, Hu Q, Nakamura Y, Lee J, Zhang G, From AH, Zhang J. The role of the sca-1+/CD31- cardiac progenitor cell population in postinfarction left ventricular remodeling. *Stem Cells.* 2006;24:1779-1788.
7. Chen X, Piacentino V, 3rd, Furukawa S, Goldman B, Margulies KB, Houser SR. L-type Ca²⁺ channel density and regulation are altered in failing human ventricular myocytes and recover after support with mechanical assist devices. *Circ Res.* 2002;91:517-524.
8. Chen X, Zhang X, Kubo H, Harris DM, Mills GD, Moyer J, Berretta R, Potts ST, Marsh JD, Houser SR. Ca²⁺ influx-induced sarcoplasmic reticulum Ca²⁺ overload causes mitochondrial-dependent apoptosis in ventricular myocytes. *Circ Res.* 2005;97:1009-1017.
9. DiPaola K, Mattiello JA, Jeevanandam V, Houser SR, Margulies KB. Myocyte recovery after mechanical circulatory support in humans with end-stage heart failure. *Circulation.* 1998;97:2316-2322.
10. Harris DM, Mills GD, Chen X, Kubo H, Berretta RM, Votaw VS, Santana LF, Houser SR. Alterations in early action potential repolarization causes localized failure of sarcoplasmic reticulum Ca²⁺ release. *Circ Res.* 2005;96:543-550.

Adolescent Feline Heart Contains a Population of Small, Proliferative Ventricular Myocytes With Immature Physiological Properties

Xiongwen Chen, Rachel M. Wilson, Hajime Kubo, Remus M. Berretta, David M. Harris, Xiaoying Zhang, Naser Jaleel, Scott M. MacDonnell, Claudia Bearzi, Jochen Tillmanns, Irina Trofimova, Toru Hosoda, Federico Mosna, Leanne Cribbs, Annarosa Leri, Jan Kajstura, Piero Anversa and Steven R. Houser

Circ Res. 2007;100:536-544; originally published online February 1, 2007;

doi: 10.1161/01.RES.0000259560.39234.99

Circulation Research is published by the American Heart Association, 7272 Greenville Avenue, Dallas, TX 75231

Copyright © 2007 American Heart Association, Inc. All rights reserved.

Print ISSN: 0009-7330. Online ISSN: 1524-4571

The online version of this article, along with updated information and services, is located on the World Wide Web at:

<http://circres.ahajournals.org/content/100/4/536>

Data Supplement (unedited) at:

<http://circres.ahajournals.org/content/suppl/2007/02/01/01.RES.0000259560.39234.99.DC1.html>

Permissions: Requests for permissions to reproduce figures, tables, or portions of articles originally published in *Circulation Research* can be obtained via RightsLink, a service of the Copyright Clearance Center, not the Editorial Office. Once the online version of the published article for which permission is being requested is located, click Request Permissions in the middle column of the Web page under Services. Further information about this process is available in the [Permissions and Rights Question and Answer](#) document.

Reprints: Information about reprints can be found online at:

<http://www.lww.com/reprints>

Subscriptions: Information about subscribing to *Circulation Research* is online at:

<http://circres.ahajournals.org/subscriptions/>